Multilevel reflectance switching of ultrathin phase-change films

Yimam, D. T.; Vermeulen, P. A.; Loi, M. A.; Kooi, B. J.

Link to publication in University of Groningen/UMCG research database

Multilevel reflectance switching of ultrathin phase-change films

P. A. Vermeulen [ID], D. T. Yimam [ID], M. A. Loi [ID], and B. J. Kooi

View Online   Export Citation   CrossMark

ARTICLES YOU MAY BE INTERESTED IN

Multilevel reflectance switching of ultrathin phase-change films

View Online   Export Citation   CrossMark

P. A. Vermeulen,[a)] (iD) D. T. Yimam,[a)] (iD) M. A. Loi, (iD) and B. J. Kooi[b)]

AFFILIATIONS

Zernike Institute for Advanced Materials, Nijenborgh 4, 9747 AG Groningen, The Netherlands

[a)]**Contributions:** P. A. Vermeulen and D. T. Yimam contributed equally to this work.
[b)]**Author to whom correspondence should be addressed:** b.j.kooi@rug.nl

ABSTRACT

Several design techniques for engineering the visible optical and near-infrared response of a thin film are explored. These designs require optically active and absorbing materials and should be easily grown on a large scale. Switchable chalcogenide phase-change material heterostructures with three active layers are grown here using pulsed laser deposition. Both Fabry–Perot and strong interference principles are explored to tune the reflectance. Robust multilevel switching is demonstrated for both principles using dynamic ellipsometry, and measured reflectance profiles agree well with simulations. We find, however, that switching the bottom layer of a three-layer device does not yield a significant change in reflectance, indicating a maximum in accessible levels. The pulsed laser deposition films grown show promise for optical display applications, with three shown reflectance levels.

INTRODUCTION

Thin optical coatings are used in displays, sensors, and communication and data transfer devices. While each application has different requirements concerning performance parameters, we may identify several desirable features regardless: systems should be small (or thin), lightweight, give high contrast, and the working wavelength should be tunable. To this end, nanometer-thin coatings with various absorptive, reflective, and even switchable characteristics are being researched.

The field of nanometer thickness absorbing optical coatings was opened by Kats et al.[1] who demonstrated reflectance color tuning of a coating of a few nanometers absorbing dielectric layer (Ge) on a metallic reflector (Au). The coatings allowed for a tunable reflection peak throughout the visible spectrum, with decent reflectance peak maxima at 40%–80% of incident light. They dubbed this the "strong interference" effect, since the light is only interfering within the thin lossy dielectric. Due to the far subwavelength layer thickness, most phase shift is accumulated on reflection at the interfaces, which makes the reflectance profile robust under tilted incidence.[1] These thickness determined colors are therefore sometimes referred to as structural colors. Later reports include similar experiments using various substrates (like paper), different absorber layers,[2,3] and even phase-change material (PCM) films.[4–7]

Hosseini et al.[8] showed a different device geometry, using the switchable phase-change material $Ge_2Sb_2Te_5$ (GST) stacked on a relatively thick oxide layer (ITO) and a bottom reflector (Pt). The thick oxide provides a resonance cavity with effectively zero absorption, which allows phase accumulation and interference due to travel between top (GST) and bottom (Pt) reflectors, commonly dubbed "Fabry–Perot" interference. Similar reflectance intensities can be reached, and importantly, Hosseini et al. show switching the GST to the crystalline state yields a distinct change in the reflectance profile. Using nanopatterning, and by leaving out the bottom reflector, they demonstrate the feasibility of transparent, flexible, electronically switchable displays. While the optical reflectance profiles might exhibit only subtle peak and intensity shifts, the human eye is relatively sensitive to these 10–20 nm color shifts. With the appropriate choice for a given application, optical displays made from these heterostructures may rival those of organic light-emitting diode (OLED) displays.[8]

Finally, Yoo et al.[9] sought to combine both interference mechanisms, introducing a bottom reflector (Pt), a resonant ITO layer, followed by a bilayer of GST, separated by a thermal barrier oxide which should allow for separate switchability of both GST layers. The major reflection resonance tuning is achieved through the ITO thickness (~200 nm). By (partially) crystallizing the bilayer, the resonance peak will shift, similar to Hosseini et al. Similar results were

obtained by using a bilayer of Sb_2Te_3 and GeTe, but the authors did not separate the layers by a diffusion barrier, which is problematic for reversible operation.[10] Many authors have followed the path of introducing nanopatterning either within the phase-change or reflector layer to make use of plasmon resonance frequencies, but this introduces a still poorly understood level of complexity, both in terms of analysis and device fabrication.

Phase-change materials (PCMs) such as GeTe, Sb_2Te_3, and GST are widely used in data storage, i.e., CDs DVDs, Blu-ray discs, and also phase-change random access memory. These applications fundamentally depend on the repeated and fast (nanosecond) reversible switching of their PCM layers. Reversibility, by switching back to the amorphous phase, is well documented in the literature and is accomplished using a small-volume element which is first melted and then rapidly cooled to avoid crystallization. The use of small area films precludes analysis using ellipsometry or reflectometry, however.

In this work, we compare the reflectance curves of both Fabry–Perot and strong interference multilevel switchable systems, incorporating three different PCMs with distinctly different crystallization temperatures. We demonstrate that the layers crystallize separately using dynamic ellipsometry and show the reflectance profile changes distinctly for each level, allowing multiple states to be robustly accessed.

EXPERIMENTAL

Films were grown using pulsed laser deposition (PLD). Thin films of $Ge_2Sb_2Te_5$ (GST), Sb_2Te_3, and GeTe were deposited on Si/SiO_2 substrates at room temperature, yielding amorphous films as confirmed by reflective high-energy electron diffraction (RHEED). The films were grown using a KrF (248 nm) laser, energy density of 1 Jcm^{-2}, at 1 Hz pulse rate. The deposition chamber was kept at 0.12 mBar inert Argon gas and a base pressure $<10^{-7}$ mBar. Roughness varied slightly between films but was generally extremely smooth with RMS values below 1 nm. Exact heterostructure stackings are given for all results. Thin (3–4 nm) spacer layers of $LaAlO_3$ (LAO) were used in-between and on top of phase-change material (PCM) and metal layers to prevent intermixing and evaporation during heating. Sample composition was verified using an FEI Nova NanoSEM

Scanning Electron Microscope and Electron-Dispersive Spectroscope (SEM-EDS). Layer thickness was determined by scratching the samples and measuring thickness using a Bruker Veeco Multimode 8 atomic force microscope (AFM). Ellipsometry was performed with a J. Woollam UV-VIS spectroscopic ellipsometer and the VASE software was used to determine optical parameters and verify the thickness of all films and heterostructures.

To extract the refractive index of layers, measurement data of ψ and Δ for both as-deposited and crystallized samples of PCM thin films were gathered in the spectrum range of 300–1700 nm with steps of 10 nm using variable angle spectroscopic ellipsometry (VASE). Reflection spectra were collected at 65°, 70°, and 75° which significantly improve measurement and fitting accuracy.

For the dynamic ellipsometry measurements, we used the HTC-100 heating stage controlled by the TempRampVASE software. The heating cell is attached to the VASE setup. All dynamic ellipsometry measurements were conducted at 70° angle of incidence, since this is the only angle available when using the heating cell.

The optical properties of transparent oxides (LAO and SiO) were fitted using a standard Cauchy model. A 1-oscillator Tauc–Lorentz model was used for amorphous PCMs, and a Drude conduction term was added to this to describe metals and crystalline PCMs. Low mean squared error (MSE) error fits were obtained in all cases. Theoretical multilayer reflectance profiles were calculated using an in-house developed script based on the Fresnel equations and a Transfer Matrix algorithm.[11,12] For dynamic ellipsometry in multilevel systems, the observed Ψ and Δ parameters are directly plotted, which can be related to the reflectance according to $\tan\Psi\cos\Delta = R_p/R_s$, where Ψ gives the amplitude ratio, Δ is the phase offset between p- and s- polarized light, and R_p and R_s are the reflected intensities of both polarizations.[13]

The reflectance for most of our samples was carried out by a custom made setup. Two optical fibers were pointed at the samples: one for a broad-spectrum white-light source and another for the analyzer. Both optical fibers are attached to goniometers to allow varying angle of incidence. The reflection spectrum is analyzed using a spectral analyzer and normalized to reflection off a reference wafer. For the samples analyzed using

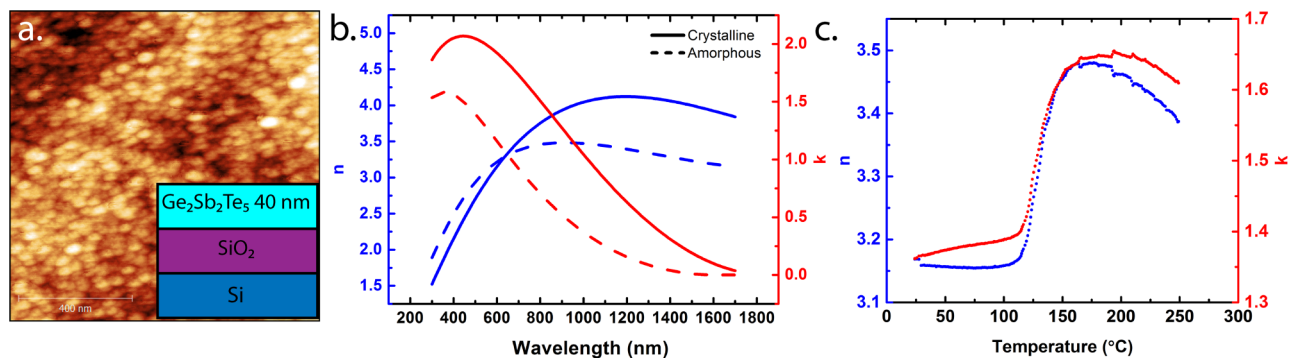**FIG. 1.** (a) AFM scan (1 × 1 μm^2 area) of 40 nm GST film with an RMS roughness of 0.8 nm. The inset schematically shows the layer geometry. (b) Real part n and imaginary or absorptive part k of dielectric function obtained using ellipsometry. (c) The pseudo n and k values during heating of the GST film are obtained using dynamic ellipsometry at 630 nm. The crystallization is clearly observed between 120 and 150 °C.
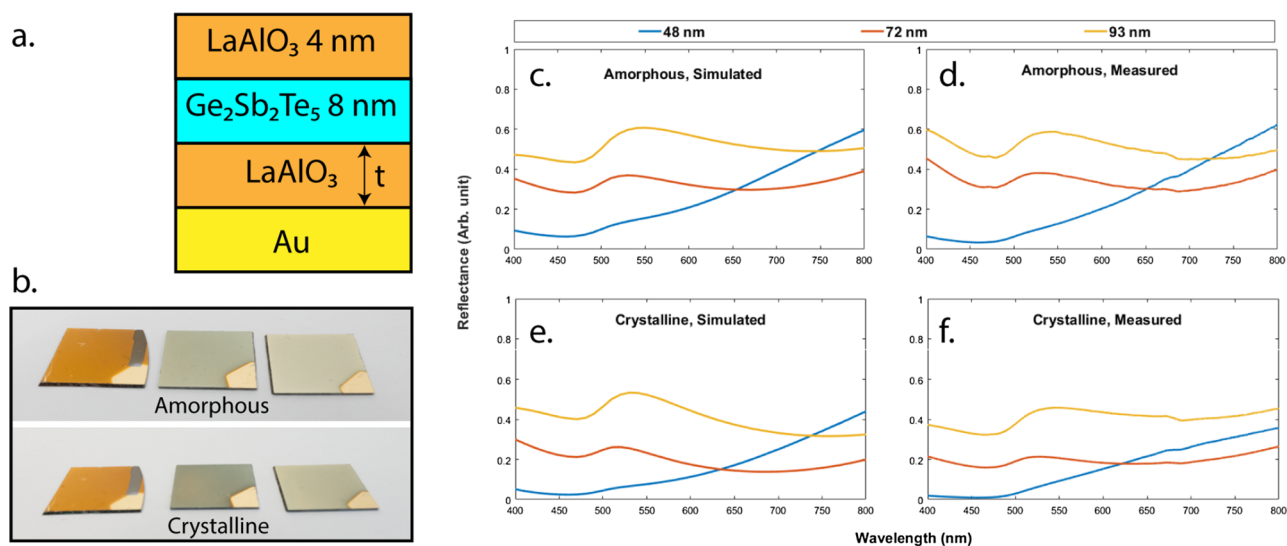
FIG. 2. (a) Geometry of a Fabry–Perot type optically tunable system. (b) Photograph of the samples before and after crystallization. The color changes subtly, and the reflected intensity is lower for crystalline phase. (d) and (f) The optical reflectance profiles as measured using a reflectometer compare quite well to simulated data [(c) and (e)].

dynamic ellipsometry, however, the reflectance was measured using the ellipsometer, which has a minimum incidence angle of 12°. This does not significantly change the obtained reflectance profile as is shown in Sec. 1 of the supplementary material. All reported reflectance profiles are taken from R_p.

Since our films are not separated into individual electrically accessible pixels, but instead consist of one large surface area ($1 \times 1 \, cm^2$), they cannot be fully melt-quenched. While this could be accomplished

using a laser probe, the resulting amorphous spot would be too small to be analyzed using ellipsometry.[14]

RESULTS

Figure 1(a) shows the modeled layer system as well as a typical AFM scan of a GST film surface. Using this layer structure, ellipsometry was performed before, during, and after
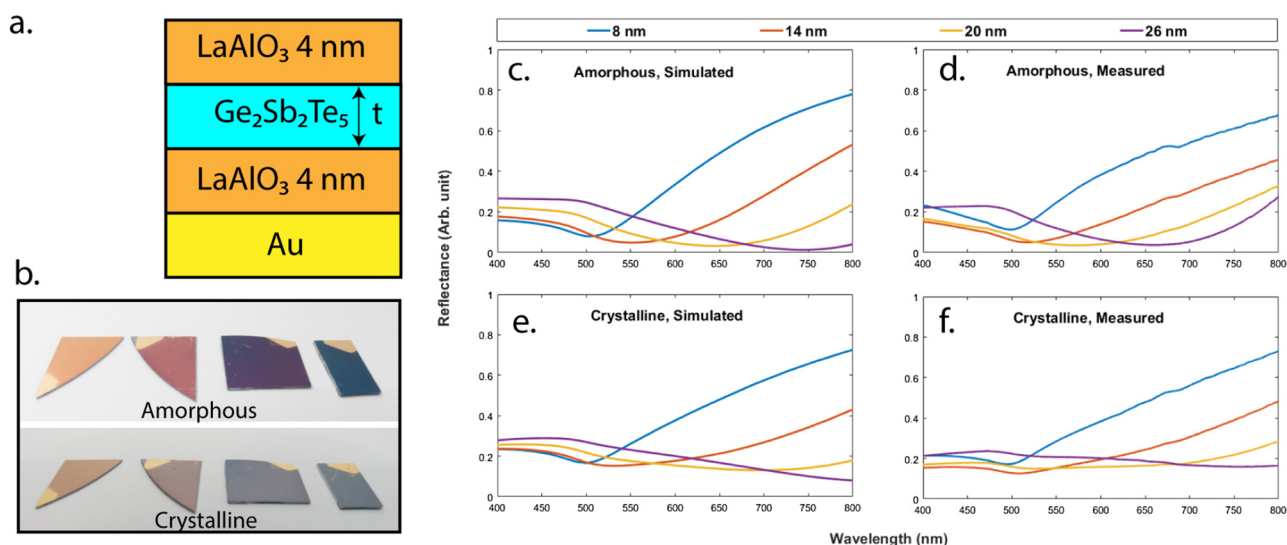

FIG. 3. (a) Geometry of a strong interference type optically tunable system. (b) Photograph of the samples before and after crystallization. The color changes are quite pronounced. (d) and (f) The optical reflectance profiles as measured using a reflectometer compare quite well to simulated data [(c) and (e)].

heating the films to 250 °C. Figure 1(b) shows the n and k values of GST before and after crystallization. From the observed dielectric parameters, we immediately see that the largest differences may be obtained in the near-infrared (NIR) region, but mainly the extinction shows a large change within the VIS region as well. Figure 1(c) shows the change in "pseudo" n and k values during crystallization. The phase transition is clearly observed as a step, allowing this dynamic ellipsometry to be used to analyze the phase transition temperature. Additional fitting results for other materials are available in Ref. 12. This extensive dataset of PLD-grown films is essential to simulate the optical response and optimize optically functional heterostructures. As mentioned in the Introduction, the optical response of a multilayer can be tuned in several ways, which we will demonstrate using two distinct geometries, starting from 2-level systems and expanding toward n-level systems.

Fabry–Perot

Fabry–Perot type interference films were grown on a 100 nm Au film, using an LAO spacer layer and GST top absorber (8 nm). A thin LAO capping layer (4 nm) prevents oxidation and evaporation. Figure 2 shows the optical response at perpendicular incidence for three LAO cavity thicknesses, for both amorphous and crystalline GST. Clear differences in the reflectance spectra are observed: maxima shift by tens of nanometers and reflected intensity shifts and drops significantly. An optical camera image shows mainly the intensity changes in red/IR are visible. The simulations match the observed data quite well.

Strong interference

To investigate strong interference, a thin film of GST is deposited on a 100 nm Au film, with 4 nm LAO on both sides, to prevent
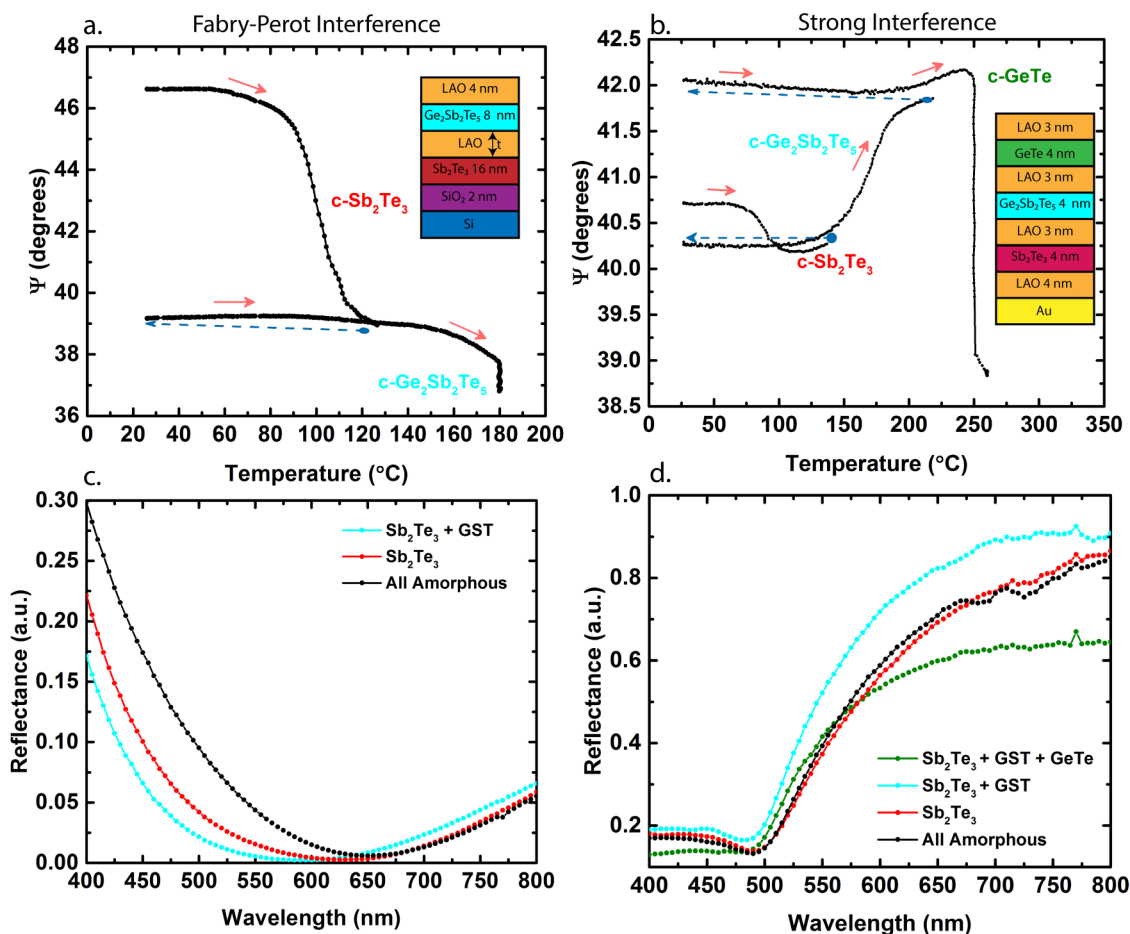
FIG. 4. (a) Dynamic ellipsometry at 630 nm of a Fabry–Perot type system with two PCM layers, and (b) strong interference type with three PCM layers. Red arrows indicate heating, and blue arrows indicate cooling. Sb_2Te_3 crystallizes around 100 °C, $Ge_2Sb_2Te_5$ around 170 °C, and GeTe around 240 °C. The crystallization events are distinctly separated, allowing easy switching and access to all substates. (c) and (d) Reflectance profiles taken using an ellipsometer with subsequently crystallized sublayers. (c) Crystallizing one or both layers redshifts the reflection by ~25 and ~50 nm. (d) Crystallizing the bottom Sb_2Te_3 layer does not significantly influence the reflectance spectrum, but all subsequent crystallization events do show a significantly altered reflectance profile, which is redshifted (GST) or blueshifted (GeTe) upon crystallization.

intermixing[10] as well as evaporation/oxidation.[15] Figure 3 shows the optical response of four films, their thickness is tuned to produce apparent reflected colors throughout the visible spectrum. Crystallizing the GST films shows a profound effect on both the spectra maximum wavelength and intensities, which leads to color and intensity changes easily visible to the eye. As for the Fabry–Perot system, the agreement between experiment and simulation is remarkably good. However, the change in apparent color upon crystallization is clearly more pronounced.

Multilevel switching

Due to the excellent agreement between simulation and experimental data and strong response of the samples to crystallization of one sublayer, a logical next step was to grow heterostructures consisting of multiple phase-change layers. Figures 4(a) and 4(b) show dynamic ellipsometry measurements, which reveal the phase transitions of Sb_2Te_3, GeTe, and GST layers within the heterostructure. The transitions are well separated, which allows for easy discrete switching in three steps. The observed values of Ψ are dependent on the exact heterostructure and, therefore, the curves of Figs. 4(a) and 4(b) cannot be directly compared; however, the change in Ψ is an indicator for change of reflectance. Figure 4(c) shows the optical reflectance of a 2-level Fabry–Perot film that significantly differs in amorphous, crystalline-amorphous, and fully crystallized levels. The reflectance minimum of the film redshifts by 50 nm upon subsequent crystallization of both sublayers. Figure 4(d) shows the optical reflectance of a 3-layer strong interference film. Crystallization of the bottom Sb_2Te_3 layer does not significantly change the reflectance profile, which makes this layer effectively inaccessible.

For the subsequent crystallization of GST and GeTe, a distinct change in reflectance in the 600–800 nm spectral range is observed. When GST and GeTe increase and decrease Ψ, they also, respectively, increase and decrease the reflectance. We find that the observed change in Ψ for Sb_2Te_3 is compensated by a change in Δ, preventing any significant change in reflectance. This is further elucidated in the supplementary material. In this case, ellipsometry reveals the crystallization, but the heterostructure interference of the p-polarized light is not significantly changed. This reduces the current film to a 3-level system. Two more 3-level Fabry–Perot devices with a thicker oxide than the one shown in Fig. 4(a) were grown. Their reflectance profiles show similar trends to the one in Fig. 4(c) and are shown in the supplementary material.

DISCUSSION

In this report, we have compared single- vs multi-PCM switchable optical devices in two different geometries. Figure 4 shows two device geometries based on two different interference schemes, working in different wavelength ranges, but both capable of accessing multiple reflectance states. The reflectance of the Fabry–Perot device is significantly lower, for comparable layer thickness. The strong interference systems should be more robust against angle-of-incidence changes. Furthermore, the layers for strong interference are generally thinner, which improves structural quality and reduces deposition times. Since our devices can only be switched by external heating, no reversible switching was demonstrated. It is impossible to transform

the high-temperature layer without transforming the low-temperature layer by heating the whole stack. The current films are a proof of concept, which show it is possible to fabricate a 2n multilayer. When the film is applied in a functional device, e.g., Hosseini et al.,[8] electrical contacts to individual layers are made through the use of a conductive oxide such as ITO. This has been proven to allow selective switching of individual layers through Joule heating.

The three-level strong interference stack did not show reflectance change when the bottom PCM was switched. The changes of Ψ and Δ are consistent both with a crystallizing sublayer and an unchanged reflectance ratio. At each interface, the initial light intensity is split into polarized reflected and transmitted intensity portion, as well as some diffusely scattered light due to roughening. For a heterostructure with a high number of interfaces and absorbing layers, the light intensity reaching the lower layers becomes very small. This means the further down a layer is, like the Sb_2Te_3, the smaller its contribution in changing the reflection profile. A similar result was reached by Yoo et al.[9] This effectively imposes a limit on the number of levels available to these kinds of systems.

CONCLUSIONS

We show high-quality multilevel switchable optical reflective heterostructure films. The films were grown using three different phase-change materials using pulsed laser deposition without nanopatterning. We observe clear reflected color and intensity changes upon crystallization of the switchable PCM layers. The phase changes were explicitly observed using dynamic ellipsometry and were well separated, allowing for discrete switching operation. Two optical interference designs were demonstrated, Fabry–Perot and strong interference, and in both configurations, the experimental results are reproduced well by the Fresnel and Transfer Matrix calculations. Both multi-PCM designs showed the expected multiple discrete optical permittivity levels; however, the reflectance of the eight-level device did not significantly change upon crystallization of the first layer.

SUPPLEMENTARY MATERIAL

See the supplementary material for Angle-dependent reflectance (Sec. 1), Dynamic ellipsometry and simulation of the 3-PCM device (Sec. 2), Additional two-PCM Fabry–Perot films and simulations (Sec. 3), and 3-PCM Fabry–Perot device simulations (Sec. 4).

ACKNOWLEDGMENTS

REFERENCES

[1] M. A. Kats, R. Blanchard, P. Genevet, and F. Capasso, "Nanometre optical coatings based on strong interference effects in highly absorbing media," Nat. Mater. **12**, 20–24 (2012).

[2] V. K. Mkhitaryan et al., "Tunable complete optical absorption in multilayer structures including $Ge_2Sb_2Te_5$ without lithographic patterns," Adv. Opt. Mater. **5**, 1–7 (2017).

[3]M. A. Kats and F. Capasso, "Optical absorbers based on strong interference in ultra-thin films," Laser Photonics Rev. **10**, 735–749 (2016).

[4]F. F. Schlich and R. Spolenak, "Strong interference in ultrathin semiconducting layers on a wide variety of substrate materials," Appl. Phys. Lett. **103**, 213112 (2013).

[5]G. Bakan, S. Ayas, T. Saidzoda, K. Celebi, and A. Dana, "Ultrathin phase-change coatings on metals for electrothermally tunable colors," Appl. Phys. Lett. **109,** 071109 (2016).

[6]Y. Meng et al., "Design of a 4-level active photonics phase change switch using VO_2 and $Ge_2Sb_2Te_5$," Appl. Phys. Lett. **113**, 071901 (2018).

[7]H.-K. Ji et al., "Non-binary colour modulation for display device based on phase change materials," Sci. Rep. **6**, 39206 (2016).

[8]P. Hosseini, C. D. Wright, and H. Bhaskaran, "An optoelectronic framework enabled by low-dimensional phase-change films," Nature **511**, 206–211 (2014).

[9]S. Yoo, T. Gwon, T. Eom, S. Kim, and C. S. Hwang, "Multicolor changeable optical coating by adopting multiple layers of ultrathin phase change material film," ACS Photonics **3**, 1265–1270 (2016).

[10]L. Lu, W. Dong, J. K. Behera, L. T. Chew, and R. E. Simpson, "Inter-diffusion of plasmonic metals and phase change materials," J. Mater. Sci. **54**, 2814 (2018); e-print arXiv:1808.08682.

[11]McGehee Group, TransferMatrix Script, Stanford Group, see https://web.stanford.edu/group/mcgehee/transfermatrix/index.html.

[12]D. T. Yimam, *Optical Properties of Pulsed Laser Deposited Telluride Heterostructures* (University of Groningen, 2018), see http://fse.studenttheses.ub.rug.nl/18477/.

[13]H. Fujiwara, *Spectroscopic Ellipsometry Principles and Applications. Spectroscopic Ellipsometry Principles and Applications* (Wiley, 2007).

[14]F. F. Schlich, P. Zalden, A. M. Lindenberg, and R. Spolenak, "Color switching with enhanced optical contrast in ultrathin phase-change materials and semiconductors induced by femtosecond laser pulses," ACS Photonics **2**, 178–182 (2015).

[15]M. T. K. Perumal, "Epitaxial growth of Ge-Sb-Te based phase change materials," Ph.D. thesis, Humboldt University of Berlin, 2013.